Available online at www.sciencedirect.com
SCIENCE DIRECT®

Catalysis Today 93–95 (2004) 235–240

CATALYSIS TODAY
www.elsevier.com/locate/cattod

Production of ammonium thiosulfate by the oxidation of hydrogen sulfide over Nb-Fe mixed oxide catalysts

Dae-Won Park [a,*], Bong-Guk Kim [a], Moon-Il Kim [a], Il Kim [a], Hee-Chul Woo [b]

[a] *Division of Chemical Engineering, Pusan National University, Pusan 609-735, Republic of Korea*
[b] *Department of Chemical Engineering, Pukyung National University, Pusan 608-739, Republic of Korea*

Abstract

The selective oxidation of hydrogen sulfide in the presence of excess water and ammonia was studied over niobium-iron mixed oxide catalysts. They showed very high conversion of H_2S with lower than 2% of SO_2 selectivity. The addition of niobium oxide to iron oxide increased H_2S conversion until Nb/Fe atomic ratio of 1/2, then the conversion decreased as the Nb/Fe ratio increased from 1/2 to 5/1. Temperature programmed techniques and XPS studies revealed that the highest activity of Nb-Fe(1/2) was due to its highest reoxidation capability. Calcination temperature also affected the performance of Nb-Fe catalyst either by changing the reoxidation property or by forming a $FeNbO_4$ phase.

Keywords: Oxidation; Hydrogen sulfide; Niobium-iron mixed oxide; Ammonium thiosulfate

1. Introduction

Since the international environmental regulations concerning the release of sulfur-containing gas become more stringent, hydrogen sulfide contained in the acid gases should be effectively recovered before emission to atmosphere. For many years, most of hydrogen sulfide in petroleum refineries and natural gas plants has been removed by the well-known Claus process [1,2]. However, due to thermodynamic limitations, typically 3–5% H_2S is not converted into sulfur. For treating a low concentration (<5 vol.%) of sulfur-containing gas in the tail gas from the Claus plant or other emission sources, various commercial processes that are based on adsorption, absorption, and wet oxidation have been used. Among the processes, the most attractive process developed during the last 20 years is the dry catalytic oxidation of H_2S to elemental sulfur after the hydrogenation of sulfur-containing gas to H_2S. Commercially developed are MODOP process [3,4], and Super Claus process [5,6].

Although the oxidation of H_2S to elemental sulfur has been widely studied [7], no work except ours has been reported for its vapor phase conversion in the presence of excess water and ammonia. The mixed gas of H_2S, NH_3, and water vapor is released from steel smelting process, where the H_2S from coke oven is generally scrubbed and concentrated using aqueous ammonia solution. The concentrated H_2S is separated from the solution and transferred to the Claus plant. However, the separation of H_2S from the solution is not perfect and the remaining aqueous ammonia stream contains about 2% H_2S which in turn causes the SO_X emission problem during incineration. Hence, new technologies are being examined to remove H_2S in this kind of stream. One approach is the selective catalytic oxidation of H_2S to elemental sulfur and ammonium thiosulfate (ATS: $(NH_4)_2S_2O_3$).

We reported a new vapor phase catalytic process for the selective conversion of H_2S in the stream containing both of ammonia and water [8,9]. V_2O_5/SiO_2 and Co_3O_4/SiO_2 catalysts showed good catalytic activities in the selective oxidation of the H_2S to ammonium thiosulfate (ATS) and elemental sulfur. ATS has been used in photography and agricultural application. Commercial processes currently practiced for its mass production are mainly based upon the direct reaction of ammonium sulfite (AS: $(NH_4)_2SO_3$) with excess sulfur at 85–110 °C [10]. An alternative synthesis method is an aqua-ammonia base system [11], where sulfur dioxide of the Claus tail gas process is first absorbed in aqueous ammonia solution to form ammonium sulfite and ammonium

---

* Corresponding author. Tel.: +82 51 510 2399; fax: +82 51 512 8563.
E-mail address: dwpark@pusan.ac.kr (D.-W. Park).

0920-5861/$ – see front matter © 2004 Elsevier B.V. All rights reserved.
doi:10.1016/j.cattod.2004.06.047

bisulfite (ABS: NH_4HSO_3) and then H_2S gas is sparged into the reactor to produce ATS. Therefore, this new vapor phase process for the conversion of H_2S to ATS and sulfur seems to offer an advantage of simple operation.

Niobium compounds exhibit special properties not shown by the compounds of its neighbors (V, Zr, Mo, Ta) in the periodic table of elements. Therefore, the research and development on the catalytic application of niobium compounds have been very active for the last 20 years. Recently, Ziolek [12] and Tanabe [13] reviewed the catalytic application of niobium compounds. Niobium oxides remarkably enhance catalytic activity and extend catalyst life when small amounts are added to known catalysts. Mixed oxides including Nb_2O_5-SiO_2, Nb_2O_5-Al_2O_3, Nb-zeolite, mesoporous Nb-MCM-41, Nb-layer compounds have been reported to posses redox property, acidic property and/or photosensitivity [13]. Tanabe and Okazaki [14,15] observed a considerable increase of NO conversion when a small amount of Nb_2O_5 was added to Fe_2O_3 for the removal of NO by decomposition using ammonia as a reducing agent.

In this paper, we wish to report that Nb_2O_5-Fe_2O_3 mixed oxides are good catalysts for the selective oxidation of hydrogen sulfide containing excess water and ammonia. The redox properties are mainly discussed to better explain the catalytic behavior of the mixed oxides.

2. Experimental

2.1. Preparation of catalysts

The binary oxides of the niobium-iron with seven different atomic ratios (Nb/Fe = 1/0, 5/1, 3/1, 1/1, 1/2, 1/5, 0/1) were prepared by a coprecipitation method. Niobium pentachloride $NbCl_5$ (99%, Aldrich) and iron nitrate $Fe(NO_3)_3{\cdot}9H_2O$ (99.5%, Katayama Chemical Company) were used as precursors. Mixtures of 0.1 M solutions of niobium pentachloride in methanol and iron nitrate in water were hydrolyzed at pH = 6–7 by slowly adding 6N aqueous ammonia solution with continuous stirring, followed by aging at room temperature for 2 h. The precipitates were filtered, and dried at 110 °C for overnight before calcining in air at a range of temperature from 450 to 800 °C for 2 h. The catalyst was designated as Nb-Fe(*x*/*y*) where *x*/*y* is atomic ratio of Nb to Fe used for the preparation of catalysts.

2.2. Characterization of catalysts

The surface area of the individual oxides and binary mixtures was measured by N_2 adsorption method using the BET technique (Micromeritics ASAP 2000). The phase analysis was performed by X-ray diffraction crystallography with Cu Kα radiation (Rigaku, DMAX 2400). The 2θ range between 5° and 90° was scanned at a rate of 2°/min. Identification of the phases was carried out by using JCPDS data base. XPS analyses were performed with a X-ray photoelectron spectrometer (VG, ESCALAB 220) with monochromatic Al Kα radiation. The samples were pressed into self-supporting wafers without any binder, followed by a pretreatment at an ultrahigh vacuum. The binding energies were calculated using the C 1s band as reference (284.6 eV). The recorded spectra were decomposed using a least squares fitting routine program. Fe $2p_{3/2}$ and Nb $3d_{5/2}$ were used for the calculation of Fe and Nb, respectively. In order to investigate the phase cooperation mechanism, temperature programmed reduction (TPR) was carried out. Before reduction, samples were pretreated by heating under air flow from 25 to 450 °C at 10 °C/min. Reduction was achieved under a H_2/N_2 gas mixture (10 vol.% H_2). Gas flow was 20 mL/min and temperature program was from 25 to 700 °C at a heating rate of 10 °C/min. After TPR experiment, the same sample was instantly tested in temperature programmed oxidation (TPO) under 2.5 vol.% O_2 with helium gas balance. The amount of consumed H_2 and O_2 was detected by mass spectroscopy (VG Quadrupole).

2.3. Reactivity test

Reaction tests were carried out in a continuous flow fixed-bed reactor. The reactor was made of a Pyrex® tube with an ID of 1 in. A condenser was attached at the effluent side of the reactor, and its temperature was constantly maintained at 110 °C to condense only solid products (sulfur + ammonium thiosulfate). A line filter was installed after the condenser to trap any solid mist which had not been captured by the condenser. From the condenser up to the gas chromatograph, all the lines and fittings were heated above 120 °C to prevent condensation of water vapor. The flow rate of gas was controlled by a mass flow controller (Brooks MFC 5850E). Water vapor was introduced to the reactant stream using a stream evaporator filled with small glass beads, and its amount was controlled by a syringe pump. In a typical experiment the reactant mixture is consisted of 5 vol.% H_2S, 2.5 vol.% O_2, 5 vol.% NH_3, 60 vol.% H_2O (vapor) and the balance helium.

The content of effluent gas was analyzed by a gas chromatograph (HP 5890) equipped with a thermal conductivity detector and a 1.8 m Porapak T column (80–100 mesh) at 100 °C. The exit gas from the analyzer was passed through a trap containing a concentrated NaOH solution and vented out to a hood. The conversion of H_2S and the selectivity to SO_2, S and ATS are defined as follows:

$$\text{conversion of } H_2S\ (X) = \frac{[H_2S]_{\text{inlet}}[H_2S]_{\text{outlet}}}{[H_2S]_{\text{inlet}}} \times 100\ (\%)$$

$$\text{selectivity } (S) \text{ to a special product } (SO_2, S, ATS) = \frac{[\text{product}]_{\text{outlet}}}{[H_2S]_{\text{intlet}} - [H_2S]_{\text{outlet}}} \times 100\ (\%)$$

For the calculation of ATS selectivity, moles of ATS was multiplied by a factor of 2 because 1 mol of ATS can be obtained from 2 mol of H_2S.

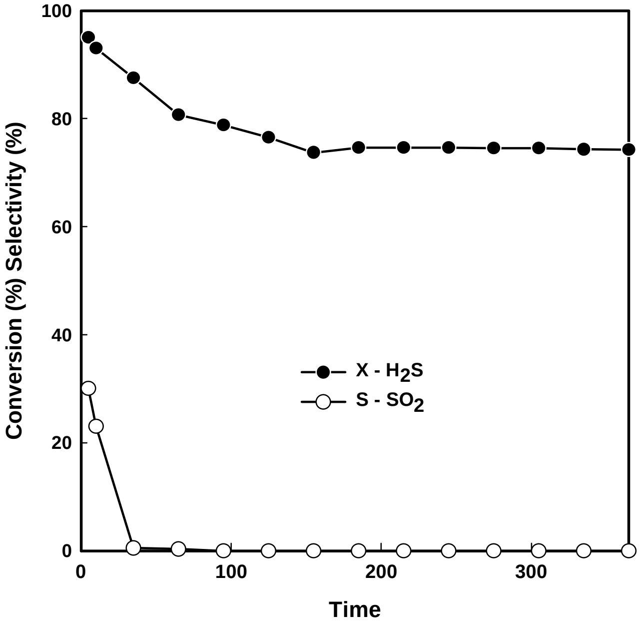

Fig. 1. Time variant conversion of H_2S and selectivity to SO_2 for Fe_2O_3 at 260 °C.

3. Results and discussion

3.1. Reaction over Fe_2O_3

In order to understand the role of Nb_2O_5 in Nb-Fe mixed oxide catalysts, pure Fe_2O_3 was first investigated for its behavior in the selective oxidation of H_2S. Fig. 1 shows time variant conversion and selectivity to SO_2. Fresh bulk Fe_2O_3 showed over than 93% of H_2S conversion during the beginning 10 min, and the conversion decreased slowly as time proceeded. After 6 h of reaction, the conversion was 77.7% and the selectivity to SO_2 was 1.8%. It is interesting to note that SO_2 production is quite high at the beginning of the reaction (30% at 5 min). As will be discussed later, this SO_2 production comes from the oxidation of H_2S with excess oxygen ($H_2S + (3/2)O_2 \rightarrow SO_2 + H_2O$) or from the oxidation of sulfur with oxygen ($S + O_2 \rightarrow SO_2$). In our previous work on the selective oxidation of H_2S over V_2O_5 [16], we reported that an oxidized form of vanadium having very active surface oxygen produced only SO_2. When V_2O_5 was reduced to a suboxide after the reaction with H_2S, the production of SO_2 decreased and only sulfur was produced when labile oxygen in vanadium was depleted by the treatment with pure hydrogen sulfide.

3.2. Characterization of Nb-Fe catalysts

Table 1 shows physical properties of Nb-Fe catalysts. Among the Nb-Fe mixed oxide catalysts, Nb-Fe(1/2) showed the highest surface area and pore volume. Nb-Fe(1/1) catalysts with different calcination temperatures (550, 650, 750 °C) showed that the increase of calcination temperature resulted in a decrease of surface area and an increase of pore size probably due to the agglomeration of catalyst particle.

Table 1
Physical properties of Nb-Fe catalysts

Catalyst	Calcination temperature (°C)	BET area (m^2/g)	Pore volume (cm^3/g)	Pore size (nm)
α-Fe_2O_3	550	19.0	–	–
Nb-Fe(1/5)	550	16.7	0.16	40.4
Nb-Fe(1/2)	550	54.8	0.32	23.0
Nb-Fe(1/1)	550	33.3	0.22	26.0
Nb-Fe(1/1)	650	22.1	0.19	34.2
Nb-Fe(1/1)	750	17.3	0.21	49.6
Nb-Fe(3/1)	550	38.4	0.12	12.6
Nb-Fe(5/1)	550	36.4	0.19	20.7
Nb_2O_5	550	67.0	–	–

Fig. 2 shows XRD patterns of Nb-Fe catalysts. Nb-Fe(1/1) catalyst calcined at 550 °C remained amorphous. Fine particles of NbO_x and FeO_x of this catalyst can not be detected by XRD. On the other hand, Nb-Fe(5/1) and Nb-Fe(1/5) showed some peaks corresponding pure Nb_2O_5 and α-Fe_2O_3, respectively. When the calcination temperature increased, some small peaks due to $FeNbO_4$ could be observed for the Nb-Fe(1/1) calcined at 650 °C, and sharp peaks of $FeNbO_4$ were observed for the catalyst calcined at 750 °C. Ananta et al. [17] also reported that the main phase of the Nb-Fe mixed oxide prepared by the solid state reaction, followed by the calcination over 1050 °C, was $FeNbO_4$.

Fig. 3 shows the surface composition ratio of Nb/Fe for fresh Nb-Fe catalysts from XPS analysis with respect to the ratio of Nb/Fe for the preparation of the catalyst. Nb component was accumulated on the surface of the catalyst. From the result of XRD and XPS, one can suggest that micro particle of Nb_2O_5 might be formed on FeO_x particles and might prevent the aggregation and crystallization of iron oxide particles. The enrichment of Nb on the surface for the Nb-Fe mixed oxide was also reported by Okazaki et al. [15].

3.3. Reaction over Nb-Fe catalysts

Five Nb-Fe catalysts of different Nb/Fe atomic ratio, and pure α-Fe_2O_3 and Nb_2O_5 were tested for the selective oxidation of hydrogen sulfide at 260 °C with feed composition of $H_2S/O_2/NH_3/H_2O/He = 5/2.5/5/60/27.5$ in vol.% and GHSV of 30 000 h^{-1}. These data were obtained after 6 h of the reaction. Table 2 summarizes the conversion of H_2S and selectivities to S, SO_2 and ATS. By the addition of small amount of Fe to Nb, the H_2S conversion increased. Nb-Fe(1/2) catalysts showed the highest H_2S conversion. The H_2S conversion decreased as the atomic ratio of Nb to Fe increased from 1/2 to 5/1. All the Nb-Fe catalysts had higher selectivity of ATS than that of elemental sulfur, and they showed very low SO_2 selectivities.

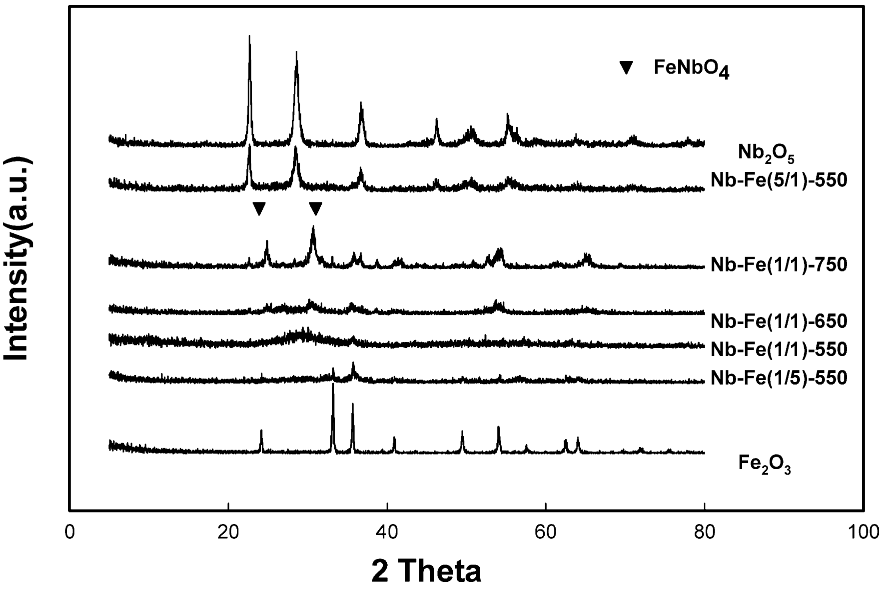

Fig. 2. XRD patterns of Nb-Fe mixed oxide catalysts.

Table 3 indicates conversion of H_2S and selectivities to S, SO_2 and ATS for Nb-Fe(1/1) catalysts with different reactant compositions. It is known that the following elementary reactions occur in the Claus process where there is no existence of ammonia and excess water [18].

$$2H_2S + O_2 \rightarrow \frac{2}{n}S_n + 2H_2O \tag{1}$$

$$\frac{1}{n}S_n + O_2 \rightarrow SO_2 \tag{2}$$

$$2H_2S + 3O_2 \rightarrow 2SO_2 + 2H_2O \tag{3}$$

$$2H_2S + SO_2 \leftrightarrow \frac{3}{n}S_n + 2H_2O \tag{4}$$

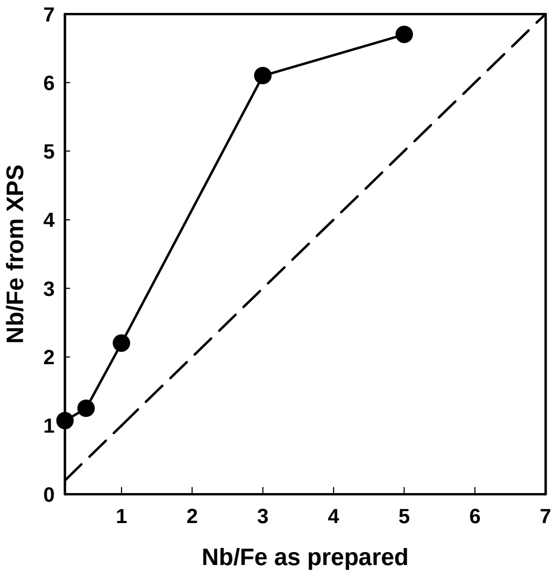

Fig. 3. Nb/Fe measured by XPS vs. Nb/Fe as prepared.

SO_2 can be produced from either consecutive reaction of elemental sulfur (Eq. (2)) or parallel reaction of H_2S with oxygen (Eq. (3)). However, when ammonia is added into reactant stream of H_2S and O_2 (Run (2)), the conversion of H_2S increases but the selectivity to SO_2 decreases compared to Run (1). This means that ammonia gas participates in the reaction with H_2S and inhibits the formation of SO_2. A separate experiment with 10% NH_3 and 2.5% H_2S (the balance helium) confirms 14.5% of H_2S conversion at 260 °C.

In the coexistence of water and ammonia (Run(3)), undesirable SO_2 emission is very small. It can be concluded from this result that water plays an important role in the reduction of SO_2, probably by accelerating the reaction of NH_3 and SO_2 as reported in a previous work [19]. A small decrease of H_2S conversion from Run (2) to Run (3) might be partially to the increase of reverse Claus reaction (4) with the presence of water vapor.

Table 4 shows the effect of calcination temperature for the Nb-Fe(1/1) catalysts with a standard reactant mixture ($H_2S/O_2/NH_3/H_2O/He$ = 5/2.5/5/60/27.5) at 260 °C. The increase of calcination temperature provoked an increase

Table 2
Conversion of H_2S and selectivities to S, SO_2 and ATS

Catalysts	*X*-H_2S (%)	*S*-SO_2 (%)	*S*-S (%)	*S*-ATS (%)
α-Fe_2O_3	68.7	0.0	25.4	74.6
Nb-Fe(1/5)	75.0	0.2	25.7	74.3
Nb-Fe(1/2)	82.4	0.8	30.0	70.0
Nb-Fe(1/1)	77.7	1.8	23.9	76.1
Nb-Fe(3/1)	75.2	2.1	36.7	63.3
Nb-Fe(5/1)	73.6	2.6	45.8	54.2
Nb_2O_5	63.6	2.8	19.8	80.2

Reaction condition: $H_2S/O_2/NH_3/H_2O/He$ = 5/2.5/5/60/27.5, GHSV = 30 000 h^{-1}, T = 260 °C, reaction time = 6 h.

Table 3
Conversion of H_2S and selectivities to special products for Nb-Fe(1/1) catalyst with different reactant compositions at 260 °C

X, S	Reactant compositions		
	(1) $H_2S + O_2$	(2) $H_2S + O_2 + NH_3$	(3) $H_2S + O_2 + NH_3 + H_2O$
X-H_2S	70.9	78.6	77.7
S-SO_2	4.8	4.1	1.8
S-S	95.2	17.5	23.9
S-ATS	–	82.5	76.1

(1) $H_2S/O_2/He = 5/2.5/92.5$; (2) $H_2S/O_2/NH_3/He = 5/2.5/5/87.5$; (3) $H_2S/O_2/NH_3/H_2O/He = 5/2.5/5/60/27.5$.

Table 4
Conversion of H_2S and selectivities to special products for Nb-Fe(1/1) catalysts calcined at different temperatures

Calcination temperature (°C)	X-H_2S (%)	S-SO_2 (%)	S-S (%)	S-ATS (%)
550	77.7	1.8	23.9	76.1
650	82.0	1.6	23.5	76.5
750	88.1	0.8	37.8	62.2

Reaction condition: $H_2S/O_2/NH_3/H_2O/He = 5/2.5/5/60/27.5$, GHSV $= 30\,000\,h^{-1}$, $T = 260\,°C$, reaction time = 6 h.

of H_2S conversion. Since high calcination temperature decreased the BET surface area, this increase of H_2S conversion might come from the formation of the $NbFeO_4$ phase as observed in Fig. 2.

3.4. Redox behaviors of Nb-Fe catalysts

In order to better understand the phase cooperation in Nb-Fe catalysts, we performed temperature programmed reduction (TPR) followed by temperature programmed oxidation (TPO). The amount of hydrogen and oxygen consumption in TPR and TPO are summarized in Table 5. All the Nb-Fe catalysts showed higher amount of oxygen consumption than bulk Fe_2O_3 and Nb_2O_5. Nb-Fe(1/2) showed maximum oxygen consumption (46.1 $\mu mol/g_{cat}$). Therefore, the highest H_2S conversion in Table 2 for this catalyst might be related to its high reoxidation capacity which participates to the reoxidation of the reduced active phase during the reaction. Nb-Fe(1/1) having the second highest H_2S conversion in Table 2 showed the second highest oxygen consumption (37.1 $\mu mol/g_{cat}$). The amount of hydrogen consumption was also high in Nb-Fe(1/2) and Nb-Fe(1/1). The amount of H_2 and O_2 consumption for Nb-Fe(1/1) catalysts at different calcination temperatures are also compared in Table 5. The catalyst calcined at 750 °C showed the highest amount of H_2 and O_2 consumption. Therefore, the highest H_2S conversion for this catalyst among the three Nb-Fe(1/1) in Table 4 can also be ascribed to its higher redox capability. From these results, one can conclude that the catalytic activity of the Nb-Fe catalysts are highly related to their redox properties.

Table 5
The amount of hydrogen and oxygen consumption in TPR and TPO experiment for Nb-Fe catalysts

Catalyst	Calcination temperature (°C)	H_2 ($\mu mol/g_{cat}$)	O_2 ($\mu mol/g_{cat}$)
α-Fe_2O_3	550	51.3	20.0
Nb-Fe(1/5)	550	53.8	25.5
Nb-Fe(1/2)	550	75.5	46.1
Nb-Fe(1/1)	550	75.6	37.1
Nb-Fe(3/1)	550	57.7	25.7
Nb-Fe(5/1)	550	49.8	21.4
Nb_2O_5	550	48.7	10.1
Nb-Fe(1/1)	650	84.6	48.3
Nb-Fe(1/1)	750	85.1	51.7

The oxidation state of Fe and Nb in Nb-Fe catalysts is studied by XPS. Fig. 4 shows XPS spectra of Fe $2p_{3/2}$ for Nb-Fe(1/2) and Nb-Fe(1/1) before and after 6 h reaction at 260 °C with the standard mixture. The XPS peaks of Fe $2p_{3/2}$ for Fe_2O_3 and FeO are located at 711.0 and 709.9 eV, respectively. After reaction the XPS spectra were broadened and shifted to lower binding energy position. It means that some of the fresh Fe_2O_3 phase having Fe^{3+} state is reduced to Fe^{2+} after the reaction. The full-width half-maximum (FWHM) value for the Nb-Fe(1/2) was 3.09 eV, and that for used one was 3.50 eV. This corresponds to 13.3% increase in FWHM after reaction. However, Nb-Fe(3/1) catalyst showed 2.18 eV for fresh catalyst and 3.47 eV for the used catalyst,

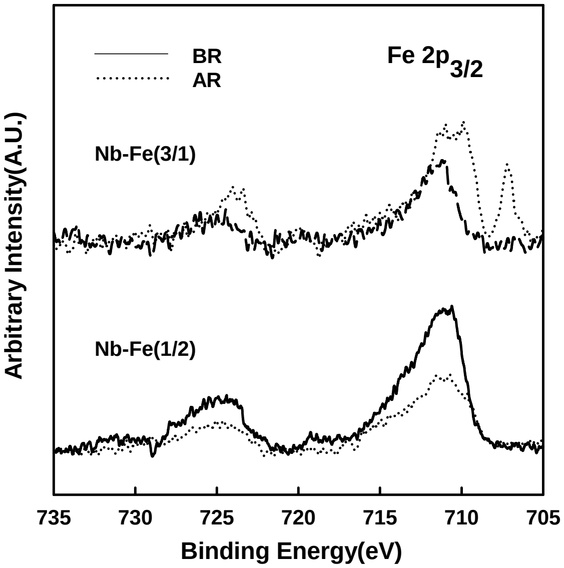

Fig. 4. XPS spectra of Fe $2p_{3/2}$ for Nb-Fe(1/2) and Nb-Fe(3/1) catalysts before reaction (BR) and after reaction (AR).

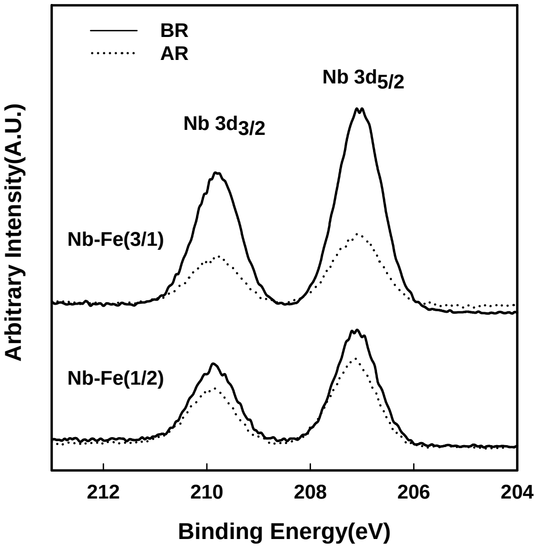

Fig. 5. XPS spectra of Nb $3d_{5/2}$ for Nb-Fe(1/2) and Nb-Fe(3/1) catalysts before reaction (BR) and after reaction (AR).

59.2% increase in FWHM. Therefore, Nb-Fe(1/2) showed less reduction of iron oxide phase during the reaction. This confirms the higher H_2S conversion of Nb-Fe(1/2) than that of Nb-Fe(3/1). It is also interesting that the peak at 707.2 eV corresponding to FeS_2 becomes significant in Nb-Fe(3/1). However, this peak was not observed in Nb-Fe(1/2). Fig. 5 shows XPS spectra of Nb $3d_{5/2}$ and $3d_{3/2}$ for the Nb-Fe(1/2) and Nb-Fe(3/1) catalysts. The oxidation state of niobium oxide was not changed significantly after the reaction.

The XPS spectra of Nb-Fe(1/1) catalysts of different calcination temperatures are compared in Fig. 6. Nb-Fe(1/1) calcined at 750 °C showed the smallest change in XPS spectrum during the reaction (an increase of 3.3% in FWHM after reaction), and it had the smallest FeS_2 peak. Table 4 showed that the Nb-Fe(1/1) calcined at 750 °C showed the highest H_2S conversion among the three catalysts. This can be explained by its higher redox capacity, and by its more stable form of iron oxide to the sulfidation.

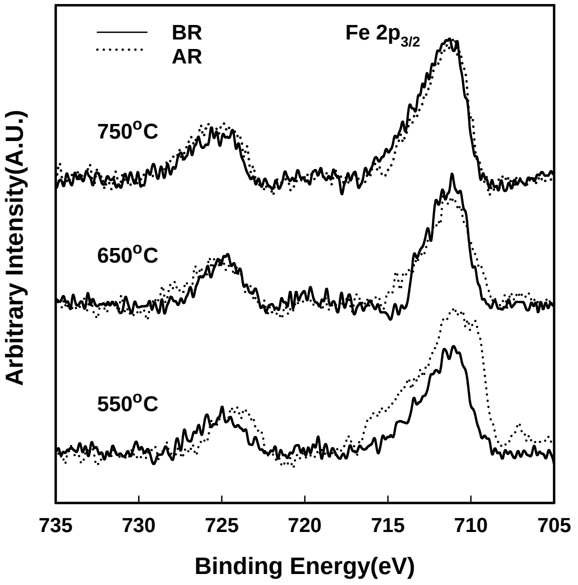

Fig. 6. XPS spectra of Fe $2p_{3/2}$ for Nb-Fe(1/1) catalysts calcined at different temperatures.

4. Conclusion

The selective oxidation of hydrogen sulfide in the presence of excess water and ammonia was investigated in this study. One can conclude that Nb-Fe mixed oxides are promising catalysts for the effective removal of hydrogen sulfide. The addition of niobium oxide to iron oxide enhanced H_2S conversion. Nb-Fe(1/2) catalyst showed the highest catalytic activity because of its high reoxidation capacity verified by TPR/TPO and XPS analyses. For Nb-Fe(1/1) catalyst, high calcination temperature decreased the surface area, but it increased the H_2S conversion probably due to its high reoxidation capacity.

Acknowledgements

This work was supported by the Korea Science and Engineering Foundation (R 05-2003-000-10050-0), and Brain Busan 21 and Brain Korea 21 program.

References

[1] R. Lell, Sulphur 178 (1985) 29.
[2] A. Pieplu, O. Saur, J.C. Lavalley, Catal. Rev. Sci. Eng. 40 (1998) 409.
[3] R. Kettner, T. Lubcke, N. Liermann, European Patent 78 690 (1983).
[4] R. Kettner, N. Liermann, Oil Gas J. 11 (1988) 63.
[5] J.A. Lagas, J. Borsboom, P.H. Berben, Oil Gas J. 10 (1988) 68.
[6] P.F.M.T. van Nisselrooy, J.A. Lagas, Catal. Today 16 (1993) 263.
[7] A. Pieplu, O. Saur, J.C. Lavalley, Catal. Rev. Sci. Eng. 40 (1998) 409.
[8] D.W. Park, S.W. Chun, J.Y. Jang, H.S. Kim, H.C. Woo, J.S. Chung, Catal. Today 44 (1998) 73.
[9] B.G. Kim, B.H. Hwang, H.S. Lee, H.C. Woo, D.W. Park, Kor. J. Chem. Eng. 21 (1) (2004) 104.
[10] K.H. Henke, G. Weiner, Ger Offen 2 635 649, 1978.
[11] A. Zey, S. White, D. Johnson, Chem. Eng. Prog. 76 (10) (1980) 76.
[12] M. Ziolek, Catal. Today 78 (2003) 47.
[13] K. Tanabe, Catal. Today 78 (2003) 65.
[14] K. Tanabe, S. Okazaki, Appl. Catal. A 133 (1995) 191.
[15] S. Okazaki, H. Kuroha, T. Okuyama, Chem. Lett. (1985) 45.
[16] Y.G. Cho, B.H. Hwang, D.W. Park, H.C. Woo, J.S. Chung, Kor. J. Chem. Eng. 19 (14) (2002) 611.
[17] S. Ananta, R. Brydson, N.W. Thomas, J. Eur. Ceram. Soc. 19 (1999) 489.
[18] S.W. Chun, J.Y. Jang, D.W. Park, H.C. Woo, J.S. Chung, Appl. Catal. B: Environ. 16 (1998) 235.
[19] B. Hsunling, B. Pratim, C.K. Tim, Ind. Eng. Chem. Fundam. 31 (1975) 88.